URSI GASS 2021, Rome, Italy, 28 August - 4 September 2021

Multi-Band Waveform-Selective Metasurfaces and Their Application

Hiroki Takeshita(1), Daisuke Nita(1), and Hiroki Wakatsuchi(1,2)
(1) Department of Electrical and Mechanical Engineering, Graduate School of Engineering,
Nagoya Institute of Technology, Nagoya, Aichi, 466-8555, Japan; e-mail: wakatsuchi.hiroki@nitech.ac.jp
(2) Precursory Research for Embryonic Science and Technology (PRESTO),
Japan Science and Technology Agency (JST), Saitama 332-0012, Japan

Abstract

In recent years, circuit-based metasurfaces containing diodes were reported to be capable of sensing a difference in different waves even at the same frequency depending on their waveforms or pulse widths. In this study, we demonstrate that such waveform-selective metasurfaces can operate at more than one frequency band. Interestingly, a proposed structure shows not only multi-band waveform-selective transmission but also an unusual response to more effectively transmit a continuous signal if the oscillation frequency is regularly switched. Potentially, our study provides a higher degree of freedom to design wireless communication environments.

1 Introduction

The advent of metamaterials made it possible to readily design a wide range of electromagnetic properties including negative refractive indices by properly tailoring their subwavelength periodic unit cells [1]. A planer type of periodic structures, or the so-called metasurfaces [2], has a simpler form and thus was so far widely used for various applications such as spatial filters [3], absorbers [4], and wavefront shaping [5]. The performances of metasurfaces are also known to be enhanced by using nonlinearities [6, 7]. For instance, circuit-based metasurfaces were recently reported using schottky diodes [8-10]. These metasurfaces distinguished different waves depending not only on the incoming frequency components like ordinary metasurfaces, but also on the waveforms, namely, on their pulse widths. Such waveform-selective metasurfaces thus gave us an additional degree of freedom to control electromagnetic waves even at the same frequency so that they were so far applied to several research fields including electromagnetic compatibility [10], antenna design [11], and signal processing [12]. However, past waveform-selective metasurfaces were restricted to a single operating frequency band, which severely limited their potential applicability. For instance, several frequency bands are used for wireless communications to enhance communication efficiency or accommodate a larger number of communication devices within a single network. For this reason, this study develops waveform-selective metasurfaces that are capable of operating at multiple frequency bands. Interestingly, a proposed structure shows not only multi-band waveform-selective transmission but also an unusual response to more effectively transmit a continuous signal if the oscillation frequency is regularly switched. Potentially, our study provides a higher degree of freedom to design wireless communication environments.

2 Materials, Theory, and Method

The fundamental mechanisms of single-band waveform-selective metasurfaces are fully explained in the literature [8-10] but can be briefly understood as follows. First of all, as drawn in Fig. 1, our metasurfaces were based on the so-called slit structures [3], which had periodic rectangular apertures or slits in a conducting sheet. In addition, each slit was connected by a set of four diodes that played a role of a diode bridge. Thus, the incoming frequency component was converted into an infinite set of components. However, the energy of the rectified waveform (i.e., |sin|) was mostly at zero frequency as calculated by its Fourier expansion [8-10]. Therefore, transient responses widely known in classic electric circuits could be exploited by deploying additional circuit components inside the diode bridge. Specifically, this study used an inductor connected to a resistor in series in each diode bridge. In this case, the electromotive force of the inductor blocked incoming electric charges during an

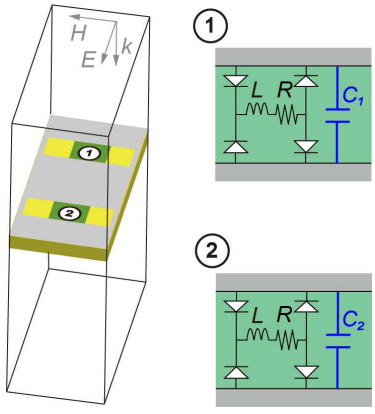

Figure 1. Super cell of dual-band waveform-selective metasurface model. Periodic boundaries were applied to the directions of the incident *E* and *H*. *L*, *R*, C_1, and C_2 were set to 1 mH, 10 Ω, 0.1 pF, and 0.6 pF, respectively.

initial time period so that the metasurface resonated like an ordinary slit structure to transmit a signal. In the case of a continuous wave (CW), however, the electromotive force almost disappeared due to the zero frequency component of rectified electric charges. For this reason, the intrinsic resonant mechanism of the slit structure was weakened for the CW even at the same frequency.

In addition, the waveform-selective metasurface used in this study was composed of two types of unit cells, each of which had an additional capacitor across the gap of each slit (see C_1 and C_2 of Fig. 1). Since the capacitors had different circuit constants, the two types of the unit cells were expected to operate at two different frequencies. Such a dual-band waveform-selective metasurface was simulated using a co-simulation method (ANSYS Electronics Desktop, 2019R3) [8-10]. To validate its experimental feasibility, we also used a measurement system that consisted of a network analyzer (Keysight Technologies, N5249A) connected to a standard rectangular waveguide (WR284) where a measurement sample was deployed.

3 Results

3.1 Waveform-Selective Metasurfaces Operating at Two Frequency Bands

Firstly, we numerically calculated transmittances of the dual-band waveform-selective metasurface model for 50-ns short pulses and CWs as plotted in Fig. 2. This figure shows that the waveform-selective metasurface had large transmittance peaks for short pulses at two different frequencies (2.4 and 3.8 GHz). At the same frequencies, however, CWs were poorly transmitted. This is because, as expected above, the transient mechanism of inductors weakened the resonances of the slits when the waveform became long enough.

Secondly, this dual-band waveform selectivity was experimentally validated. In this case, we optimized several design parameters of the measurement sample (the inset of Fig. 3) so that waveform selectivities appeared within the operating frequency band of the rectangular waveguide used. The measurement result is plotted in Fig. 3, which shows that our measurement sample more strongly transmitted short pulses near 2.6 and 3.2 GHz than CWs. This ensured the feasibility of dual-band waveform-selective metasurfaces.

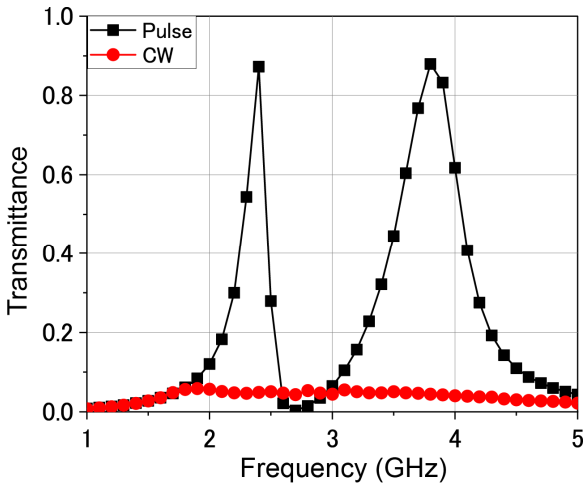

Figure 2. Simulated transmittances of the dual-band waveform-selective metasurface. The input power was set to 10 dBm.

3.2 Waveform-Selective Metasurfaces Operating at More Frequency Bands

Waveform-selective meatsurfaces can operate at more frequency bands by introducing additional cells into a super cell as drawn in Fig. 4. This super cell was composed of four types of unit cells, all of which had different capacitance values. As a result, the transmittance for a short pulse became larger than that of a CW at four

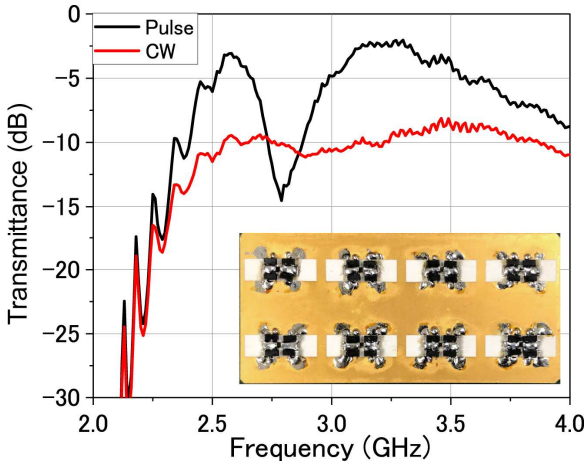

Figure 3. Measured transmittances of dual-band waveform-selective metasurface. The inset shows the measurement sample optimized for a measurement setup composed of a rectangular waveguide. The input power was set to 10 dBm.

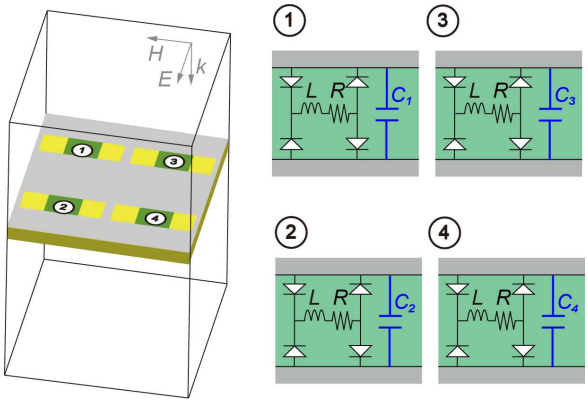

Figure 4. Super cell of four-band waveform-selective metasurface model. Periodic boundaries were applied to the directions of the incident E and H. L, R, C_1, C_2, C_3, and C_4 were set to 1 mH, 10 Ω, 0.1 pF, 0.6 pF, 0.3 pF, and 1.1 pF, respectively.

frequencies, i.e., 2.1, 2.8, 3.8, and 5.2 GHz, as seen in Fig. 5. This figure also shows that entirely the transmittances for both types of the waveforms were smaller than the transmittances of the dual-band model simulated in Fig. 2. This was in part because the spatial occupancy ratios of the unit cells were smaller than those of the dual-band unit cells.

Another important point here is that this four-band waveform-selective metasurface lowered the transmittance for a CW or a long waveform, although long signals are generally used for many practical wireless communications. However, we expected that this waveform-selective metasurface would potentially enhance its transmittance again, if the oscillation frequency of the incoming wave was regularly switched. As mentioned earlier, when a pulsed signal came in, an inductor exhibited an electromotive force. Importantly, this force related with the level of the transmittance. Also, the inductor needed a recovery time to fully restore its electric potential. We expected that this potential would come back to zero again, while the oscillation frequency was switched to other frequencies.

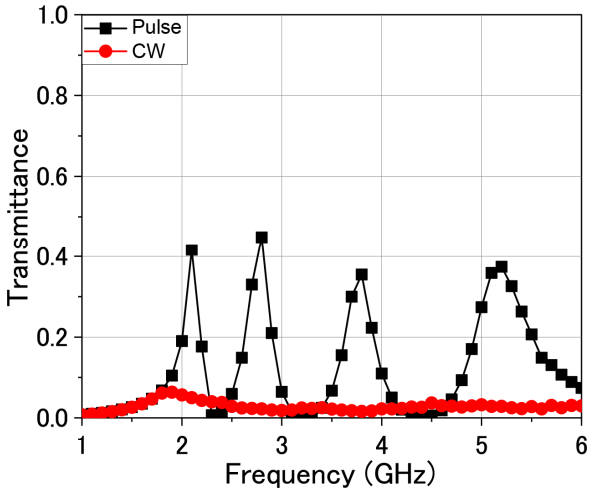

Figure 5. Simulated transmittances of the four-band waveform-selective metasurface. The input power was set to 10 dBm.

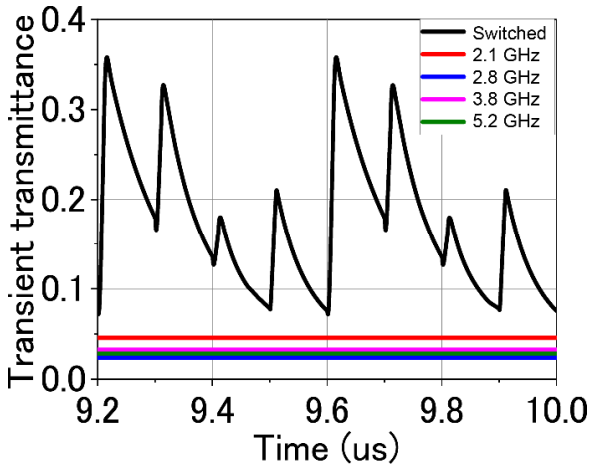

Figure 6. Transmittances of the four-band waveform-selective metasurface for a switched signal and single-frequency CWs. The switched signal periodically changed the oscillation frequency using 2.1, 2.8, 3.8, and 5.2 GHz. The input power was set to 10 dBm.

Based on this concept, the transmittance of the four-band waveform-selective metasurface for a switched signal was calculated as plotted in Fig. 6, which also includes the transmittances for individual single-frequency CW signals. As seen in this figure, the transmittance magnitude of the switched signal periodically changed depending on the original transmitting profile of the structure. However, this transmittance was markedly larger than that of any single-frequency CW signal.

4 Conclusion

In conclusion, we have demonstrated waveform-selective metasurfaces operating at more than one frequency band. Firstly, a dual-band waveform-selective metasurface was both numerically and experimentally tested so that its transmittance for a short pulse was found to be larger than that for a CW at two different frequency bands. Secondly, the concept of multi-band waveform-selective metasurface was extended to four frequency bands. This waveform-selective metasurface showed not only multi-band waveform-selective transmission but also an unusual response to more effectively transmit a continuous signal if the oscillation frequency was regularly switched. Potentially, our study is expected to provide a higher degree of freedom to design wireless communication environments.

5 Acknowledgements

This work was supported in part by the Japan Science and Technology Agency (JST) under Precursory Research for Embryonic Science and Technology (PRESTO) No. JPMJPR193A.

6 References

1. D.R. Smith, W.J. Padilla, D. C. Vier, S. C. Nemat-Nasser, and S. Schultz, “Composite Medium with Simultaneously Negative Permeability and Permittivity,” *Phys. Rev. Lett.*, 84, 4184, 2000.

2. D. Sievenpiper, L. Zhang, R.F.J. Broas, N.G. Alexopolous, and E. Yablonovitch, “High-Impedance Electromagnetic Surfaces with a Forbidden Frequency Band,” *IEEE Trans. Microw. Theory Tech.*, 47, 11, 2059, 1999.

3. H. Wakatsuchi and C. Christopoulos, “Generalized Scattering Control Using Cut-Wire-Based Metamaterials,” *Appl. Phys. Lett.*, 98, 22, 221105, 2011.

4. H. Wakatsuchi, S. Greedy, C. Christopoulos, and J. Paul, “Customised Broadband Metamaterial Absorbers

for Arbitrary Polarisation," *Opt. Express*, 18, 21, 22187, 2010.

5. N. Yu and F. Capasso, "Flat Optics with Designer Metasurfaces," *Nat. Mater*., 13, 139, 2014.

6. A.A. Zharov, I.V. Shadrivov, and Y.S. Kivshar, "Nonlinear Properties of Left-Handed Metamaterials," *Phys. Rev. Lett.*, 91, 37401, 2003.

7. A. Li, Z. Luo, H. Wakatsuchi, S. Kim, and D.F. Sievenpiper, "Nonlinear, Active, and Tunable Metasurfaces for Advanced Electromagnetics Applications," *IEEE Access*, 5, 27439, 2017.

8. H. Wakatsuchi, S. Kim, J. J. Rushton, and D. F. Sievenpiper, "Waveform-Dependent Absorbing Metasurfaces," *Phys. Rev. Lett*., 111, 24, 245501, 2013.

9. H. Wakatsuchi, D. Anzai, J. J. Rushton, F. Gao, S. Kim, and D. F. Sievenpiper, "Waveform Selectivity at the Same Frequency," *Sci. Rep.*, 5, 9639, 2015.

10. H. Wakatsuchi, J. Long, and D. Sievenpiper, "Waveform Selective Surfaces," *Adv. Funct. Mater.*, 29, 11, 1806386, 2019.

11. S. Vellucci, A. Monti, M. Barbuto, A. Toscano, and F. Bilotti, "Waveform-Selective Mantle Cloaks for Intelligent Antennas," *IEEE Trans. Antennas Propag.*, 68, 3, 1717, 2020.

12. M.F. Imania and D.R. Smith, "Temporal Microwave Ghost Imaging Using a Reconfigurable Disordered Cavity," *Appl. Phys. Lett.*, 116, 054102, 2020.